

Angström-science, angström-technology, angström-devices: A new challenge

M. POPESCU

National Institute R&D for Materials Physics, P. O. Box MG. 7, 077125 Bucharest-Magurele, Romania

Beyond nano-science is angström-science, beyond nano-technology is angström-technology, beyond nano-devices are angström-devices. Beyond these new emerging fields in materials physics is to ride on electron, but this is almost pure phantasy.

(Received February 25, 2006; accepted March 23, 2006)

Keywords: Nano-structure, Angström-structure, Graphene, Carbon tubule, Fullerene, Silicon wire, Phase change memory, Photo-structural changes, Single molecule transistor, Sub-nano-lithography, Fuel cell, Self-organization

1. Introduction

To reach the maximum of device miniaturization means to go into the intimate life of the lattices and networks of atoms, including clusters of atoms or molecules. How small could be the devices? At the limits of several angströms the material science is completely different. The practical applications of the new science lead to completely different devices. The energy consumption becomes insignificant. The electron is in strong competition with the quantum of light. The output of the devices will be mainly high quality information and not actuation as in our daily macroscopic physics. But this information will give the power to move the world.

2. Down to primary configurations of the atoms

2.1 Angström-size carbon configurations and devices

The discovery of the new world of special carbon configurations, the fullerenes, in 1985, by Kroto, Curl, Smalley and coworkers [1] (Nobel Prize in Chemistry in 1996) opened the way to a new field of chemistry and physics of the atomic networks. A fullerene, by definition, is a closed, convex cage molecule containing only hexagonal and pentagonal faces. The minimum fullerene, noted C_{60} is a round cage with 60 carbon atoms.

Stable graphene sheets have been recently reported [2]. The graphene consists of a single layer made of six-fold rings of carbon atoms.

While a simple packing of a large number of graphenes (graphite two-dimensional layers) gives rise to a dead crystal, with a limited functionality, the separated graphenes are live. The sheets of 1-2 angström thickness can be rolled, twisted, coated by various molecules, thus allowing for functional structures, to be exploited in applications. Graphene structures are template for many angström-size structures.

Andre K. Geim [3] has successfully prepared graphenes by using the mechanical exfoliation effect (repeated peeling). The graphene has metallic properties and exhibits two-dimensional ballistic electronic transport. Linear current-voltage characteristics and huge sustainable currents of over 10^8 A/cm² were reported.

Nano-tubes are giant linear fullerenes. C-C bonds have the length of 0.14 nm. The carbon nano-tubes were discovered in 1991 by Iijima [4].

To form carbon nano-tubes, an atomic planar sheet of carbon atoms is bonded together into an array of hexagons and rolled up to form molecular tubes or cylinders of diameter $10 \div 200$ Å, and length of 1-3 micrometers. The details of fabrication (the chirality) determines the electronic properties of the tube, i.e. whether the conduction is a semiconductor-like or a metallic one.

On the other hand, carbon nano-tubes of low diameter have been simulated at the atomic scale [5]. The modelling of the angström-configurations aimed to see the structural details of a tube and if it is possible its insertion in other structures or coupling with other tubes of different orientations.

Recently, the graphene was used in order to create a field effect transistor.

If graphene is used, then it is possible to fabricate a transistor in p-n-p configuration: p could be made of a silicon angström-size wire doped by group III atoms (Ga, In). The possibility to build silicon wires angström-size in diameter has been recently demonstrated by us [6]. The third terminal of the transistor connected to a small diameter carbon tube (5.83 Å) will complete the transistor (Fig. 1).

The conduction channel can be switched between two-dimensional electron and hole gases by changing the gate voltage. Postma et al. [7] have shown that the current in the tubule could be controlled at room temperature by feeding with individual electrons. In this transistor the on/off resistance ratio is under 30 at room temperature. The above value is limited because of thermally excited carriers. Fortunately, this is enough for logic circuits.

As regarding graphenes, they could be tailored from carbon nano-tubes of large diameters by cutting and rolling off the tube configuration.

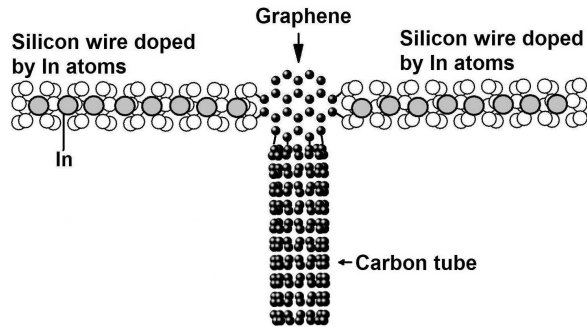


Fig. 1. An example of possible angström-structure: the *p-n-p* transistor.

The extraordinary quality of carbon, i.e. the ability to satisfy its four valence electrons by bonding with three neighbours, makes the various structures in graphenes and fullerenes possible. Each of three electrons is assigned to a partner, the fourth is shared by all of them, being delocalized all over the network. These shared electrons make fullerene aromatic and allow some nano-tubes to conduct electricity. Although the sp^2 electron configuration is convenient in a flat hexagonal tiling, rolling the sheet up expends relatively little elastic energy, which is generously returned when all the dangling, unhappy, bonds at the edges are eliminated in a seamless cylinder. The insertion of pentagon or heptagon allows for a Gaussian curvature, positive and cap-like in the case of a pentagon and negative and saddle-like where a heptagon is involved. With these two elements, all kind of equilibrium shapes and plumbing become possible in carbon construction.

The specific properties of nano-tube objects make them applicable in angström-size devices. The calculations predict the energy cost of deforming a nano-tube, and its elastic parameters agree with those known for graphite and found by first-principle theoretical methods. There were discovered humps and bumps on the strain-energy curves beyond what Hooke's law would predict that each displacement would generate a proportional restoring force. This indicated that there must be some abrupt changes in the molecule under mechanical load. Indeed, each singularity in the stress-strain curve appears to correspond to a sudden shape switch of an initial perfect cylinder. In the simulations the nano-tube is seen to snap from one shape to the next emitting acoustic waves along its walls at every "crunch". These "crunchy molecules" never actually break, but reversibly accommodate to external stress. The hollow structure is an outstanding feature of fullerene molecules and of nano-tubes in particular. As early as 18-th century, Leonhard Euler discovered the phenomenon of elastic instability. A rod or column compressed axially remains straight until a critical

force is reached. It then becomes unstable (undergoes bifurcation) and buckles sideways. The behaviour of the hollow tubules is more complex, but still predictable with continuum-elasticity methods. The laws of continuum mechanics are amazingly robust and allow one to treat even intrinsically discrete objects only a few atoms in diameter.

2.2 Angström-size phase change memory

One of the most promising media for rewritable applications is phase-change materials. The idea to use an amorphous-crystalline phase transitions for information storage dates back to the 1960s when Stanford R. Ovshinsky suggested a memory switch based on changes in the properties of amorphous and crystalline phases of multi-component chalcogenides [8].

The initial amorphous as-deposited $Ge_2Sb_2Te_5$ layer is crystallized by exposure to a laser beam of intensity sufficient to heat the material to a temperature slightly above the T_g . A subsequent exposure to an intense and short laser pulse melts the material that is then converted into the amorphous state on quenching. A recorded bit is an amorphized mark against the crystalline background. The process is reversible and this is essential for a rewritable memory.

Strand et al. [9] have shown that Ge-Te alloys having non-stoichiometric atomic ratios phase separate during crystallization into a $Te_{50}Ge_{50}$ phase plus pure crystalline tellurium or germanium. The limitation of the crystallization rate is given by this slow process of phase segregation. Phase segregation during crystallization of non-stoichiometric Ge-Te can be avoided by adding antimony to samples having a tellurium concentration of from 45 to 55 at.% over a wide range of Ge:Sb ratios. These alloys can have laser induced crystallization times of less than 50 ns.

Kolobov et al. [10] have shown the angström-scale mechanism of structural phase-change in materials, on the case of Ge-Sb-Te chalcogenide.

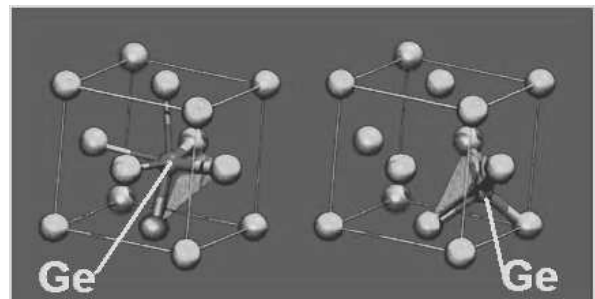


Fig. 2. Local structure of Ge-Sb-Te around germanium atoms in the crystalline (left) and amorphous (right) states [9].

In Fig. 2 (after [10]), it is shown the germanium atom in the f.c.c. structure formed by tellurium atoms. The germanium atoms occupy the octahedral and tetrahedral

symmetry positions in the crystalline and amorphous state, respectively. The stronger covalent bonds are shown with thicker lines than the weaker bonds (Fig. 2a). An intense laser pulse induces the rupture of the weak bonds and the germanium atom flips into the tetrahedral position (Fig. 2b). An alternative description of the structural transformation on melting is an umbrella flip distortion resulting in the disordering of the germanium sub-lattice. It is remarkable that the covalent bonds remain intact.

The authors conclude that Ge-Sb-Te can be viewed as being built from well-defined rigid building blocks of composition $\text{Ge}_2\text{Sb}_2\text{Te}_5$. In the crystalline state, the constraint of the mutual arrangement of the building blocks in space is such that tellurium atoms form a f.c.c. lattice. Inter-block interaction and long-range ordering cause the resulting structure to resemble the rock-salt structure. In the amorphous state, inter-block interaction is weakened, which allows the block structure to relax so that the bonds shrink and germanium umbrella flips into its preferred tetrahedral coordination.

The results presented in [10] provide a clear explanation as to why switching in Ge-Sb-Te is fast and stable and point out the power of angström-science (angström-scale phenomena). This is because the crystallization – amorphization process does not require the rupture of strong covalent bonds and the transition is diffusionless.

The fact that the tellurium sublattice is partially preserved, as well as the conservation of the antimony atoms, account for why the transformation can be easily reversed. The material does not have to be transformed into a truly liquid state. Bond rupture is believed to be due, at least partially, to electronic excitation. It also should be noted that the amorphous structure, at least on a local level, is well defined, thus enhancing the reversibility of the transition.

Welnic et al. [11] have shown that a strong difference exists between a covalent semiconductor and the prototype compound of phase-change material, $\text{Ge}_2\text{Sb}_2\text{Te}_5$.

While the covalent semiconductors have, in general, similar local arrangements, not only in crystalline, but also in amorphous phase, Ge-Sb-Te, undergoes a profound change in local order on amorphization. The last class of materials (Ge-Sb-Te) is characterized by two competing structures with similar energy but different local order and different physical properties. Both local distortions found in the crystalline phase and the occurrence of octahedral and tetrahedral coordination in the amorphous state is explained. Although the atomic rearrangement is most pronounced for germanium atoms, the strongest change of the electronic states affects the tellurium states close to the Fermi energy, resulting in a pronounced change of electronic properties such as an increased energy gap.

For some phase-change memory materials, as e.g. Si-Ge-As-Te, an angström-scale mechanism was shown in [12].

The structure of the quaternary glass $\text{Si}_{12}\text{Ge}_{10}\text{As}_{30}\text{Te}_{48}$ seems to be given by a random network of atoms linked by covalent bonds. The atoms retain the covalence known

from their crystalline compounds. Nevertheless, the As-Te bonds are favoured. The composition with 30 As and 48 Te, approaching As_2Te_3 composition, supports the idea that the main configuration in this glass is based on As_2Te_3 layers. Therefore, the idea to embed Si and Ge in As_2Te_3 layers is attractive. Interconnection of the As_2Te_3 layers containing Si and Ge atoms is possible if Si(Ge)-Te-Si(Ge) bonds are considered in-between the layers. The phase change under heat consists in the separation of the layers by breaking the interlayer bonding and releasing of Ge and Si from the As_2Te_3 layers. Thus, the new phase becomes more ordered and more stable than the initial phase. A return back to the former glassy phase is possible only by strong excitation (melting and quenching).

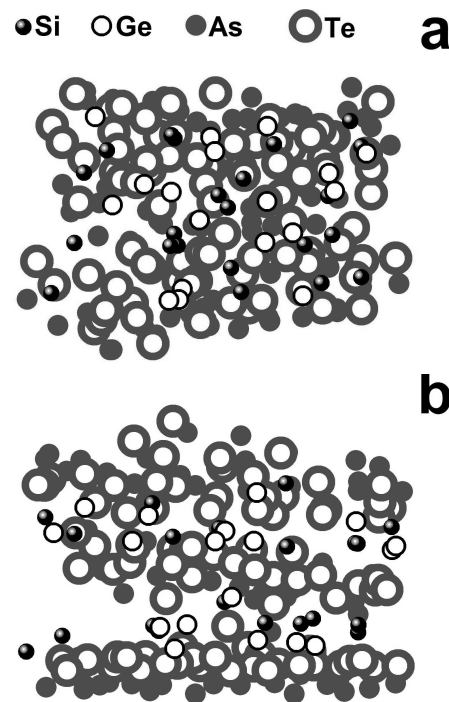


Fig. 3. Model of $\text{Si}_{12}\text{Ge}_{10}\text{As}_{30}\text{Te}_{48}$ glass (a) and the model of a new phase got by structural transformation (b).

The angström-scale model consists in an arrangement of three disordered layers of type As_2Te_3 . These layers are doped randomly with Si and Ge. The physical model made of plastic units has 202 atoms. Silicon and germanium take the places of tellurium atoms. They bind two neighbouring layers though the intermediation of the tellurium atoms released from the bonds occupied by Ge or Si. Thus, two disordered As_2Te_3 type layers are linked by square bridges Si-Te-Si(Ge)-Te. The model was relaxed by computer using the standard Monte-Carlo – Metropolis procedure and appropriate force constants. The results are shown in Fig. 3a. In the following step we modeled the phase transformation induced by external factors acting on the glass. The excitation of the stressed bonds in the glass leads to the breaking and reforming of the bonds in a new configuration. The bond breaking between disordered

layers is most probably due to stressed bonds Si-Te and Ge-Te. Tellurium takes the place of Ge (or Si) in the layers and forms strong As-Te bonds that fit the network of type As_2Te_3 . The remaining Si and Ge atoms form separated dimers or small clusters in-between the As_2Te_3 layers. The atomic scale model of the new phase, relaxed by computer is shown in Fig. 3b.

By melting and quenching, the phase obtained by annealing the glass would induce the reverse transformation to a higher free energy state.

2.3 Angström-size wires

Small angström-size tubes are good candidates for conducting wires to be used in angström-size devices.

Recently, we have simulated three types of tubular wires based on silicon. The purpose is to see if the angström-scale tubules are possible from the point of view of crystallo-chemistry. The results are shown in Fig. 4.

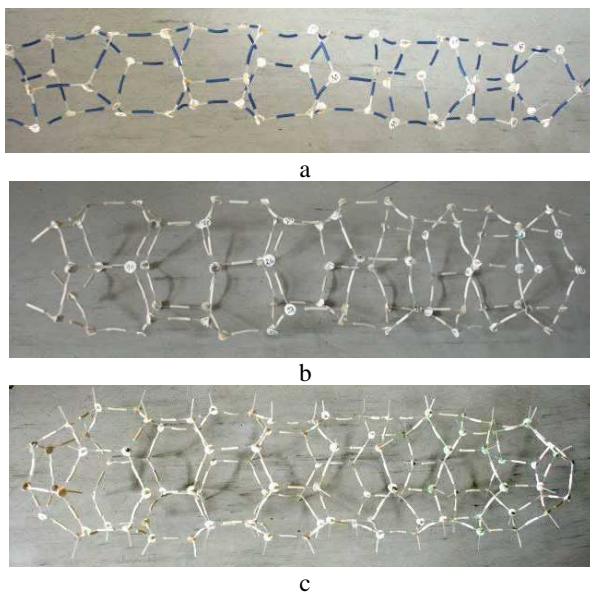


Fig. 4. The three lowest diameter silicon angström-size tubes (wires). a. small diameter: 3.8 Å, 54 atoms; b. medium diameter: 5.2 Å, 72 atoms; c. large diameter: 7.2 Å, 100 atoms

Only the silicon angström-tube of diameter 3.8 Å exhibits the correct bond angle parameter, very near to the tetrahedral angle. What is important is that the inner diameter is enough large to accommodate metal atoms.

One problem is the ends of the tube. The bonds must fit the dangling bonds of the other angström-phase to be connected with.

Recent experimental results, although not conclusive, give some indications that quantum confinement in the transverse direction of silicon nano-wires results in greater mobility than in bulk silicon [13]. Although the effect is not well understood, it seems to be related to the quantum-confined nature of the wire, which limits the density of available phonon states and hence reduces the probability

of an electron-phonon scattering event, that is, reduces the draging effect. Coupling this observation with the desirable characteristics and vast experience associated with silicon makes using silicon nano-wires as a replacement for bulk silicon channels an attractive option.

Semiconductor angström-devices composed of silicon and other materials can also function as Field Effect Transistors (FET) devices [14]. Silicon angström-wires were prepared as single crystal structures with diameters as small as 20-30 Å [15] and have been shown, for both p-type and n-type materials, to exhibit performance characteristics comparable to or better than the best achieved in the microelectronic industry [16].

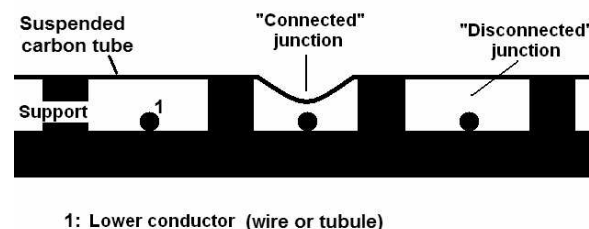
Our simulated wires have the smallest diameters possible and these are situated in the range of angströms. One of the most important features of the nano- and angström size wires is the possibility to cover the surface of the wires with different organic compounds because of the high number of dangling bonds. Thus, the silicon angström-wire is a special material, which can serve to different applications. They are able to detect species in liquid solution, as e.g. pH sensing.

The amino and silanol moieties work as receptor for hydrogen ions, undergoing protonation/deprotonation reactions, thereby changing the net nano-wire surface charge. p-type silicon nano-wires devices modified in this way exhibit stepwise increase in conductance as the pH of the solution is increased stepwise. When appropriate receptors are linked to the angström-wire active surface, then biological macromolecules, such as proteins and nucleic acids, can be easily detected.

The ultimate sensitivity of the angström-wire FET devices is the detection of viruses, and, also, of agents of biological warfare and terrorism [17].

Up to day the optical and electrical data have shown that, as a virus (e.g. influenza virus) diffuses near a nano-wire device, the conductance remains at the baseline value, and only after binding to the nano-wire surface does the conductance drops (these are field effect sensor devices).

In addition to offering some advantages compared to bulk silicon in the fabrication of FET structures, silicon nano-wires also can be used in other structures that may be better suited due to the characteristics of nano-wires such as length to diameter ratio. Cross-bar arrays are one example of these alternative structures. In such structures, one array of parallel nano-wires is overlaid on a second array of nano-wires oriented at right angles to the first array. The cross points of the arrays can be used to either store or switch information depending on the details of the device [18].



1: Lower conductor (wire or tubule)

Fig. 5. Suspended nano-wires switched connection.

The crossed nano-wires act as a switch with bi-stable positions open or closed. The mechanical equilibrium of the wires maintains the neutral (open) position. Applying opposite charges to the wires pulls them toward each other until they touch, at which time molecular forces hold them in the closed position. Applying similar charges to the two wires forces them apart, resetting them to the initial position. The performance of these isolated devices cannot in general compete with scaled silicon on speed. Their potential lies in achieving increased density and reducing fabrication costs. Proponents of cross-bar architectures argue that arrays of these devices can be “self-assembled” using fluidic assembly and Langmuir-Blodgett techniques. The major problems are in providing the gain necessary for signal restoration and fan out and to connect the self-assembled modules to global control lines.

Angstrom-wires are stable and, when combined with organic compounds can serve to detect with high sensitivity different substances in the environment. A long string of silicon atoms surrounded by organic molecules that conducts electricity, glows under ultraviolet light (becomes photo-luminescent). The polymer can be modified to behave like a “shorted-out electrical circuit” whenever it comes into contact with molecules of TNT or picric acid. This happens chemically because the TNT and picric acid (electron deficient molecules) grab electrons from the silicon polymer whenever it is excited by UV light. This prevents the silicon nano-wires from glowing. The polymer is glowing green. If TNT is added then the green luminescence of the polymer is turned off, or, in other words, the luminescence is quenched. Thus, it is possible to detect the presence of TNT down to about one part in a billion in air and some 50 parts per billion in seawater.

The narrowest feature on present-day integrated circuits is the gate oxide: the thin dielectric layer that forms the basis of field effect device structures. Silicon dioxide is the dielectric of choice and, in the near future will be thinner than one nanometer, or about five silicon atoms across. At least two of those five atoms will be at the silicon-oxide interfaces, and so will have very different electrical and optical properties from the desired bulk oxide, while constituting a significant fraction of the dielectric layer. By EELS, Muller et al. [19] measured the chemical composition and chemical structure, at the atomic scale, across gate oxides as thin as one nanometer. They resolved the interfacial states that result from the spillover of the silicon conduction band wave functions into the oxide. The spatial extent of these states places a fundamental limit of 0.7 nm (four silicon atoms across) on the thinnest usable silicon dioxide gate dielectric. And for present-day oxide growth techniques, interface roughness will raise this limit to 1.2 nm. There are two considerations: first, the roughness of the interface must be controlled at an atomic scale if such thin oxide is to prove practical. The leakage current through a 1 nm thick oxide increases by about a factor of ten for every 0.1 nm increase in the root-mean-square roughness. This leakage current, in conjunction with the sub-threshold leakage, is the most important figure of merit in a MOSFET; second, a single layer of silicon and oxygen has the incorrect topology to reproduce the local electronic structure of bulk silicon dioxide. The question is then how thick must a silicon

dioxide layer be before its bulk electrical properties can be obtained? The presence of an intrinsic transition region which may be a “sub-stoichiometric oxide”) between bulk Si and bulk-like SiO₂ will place a fundamental limit on drive current by limiting the minimum thickness. Attempts to measure the width of the transition region have given answers that range from structurally abrupt (for molecular beam epitaxy on an atomically flat substrate) to a chemical thickness of 0.3 ÷ 0.5 nm (for thermally grown oxides).

2.4 Angström-size transistor based on amorphous silicon

The amorphous silicon was demonstrated to consist of domains separated by thin or thick and more or less ordered interface [20]. The interface is a very curious feature. While we demonstrated by modeling the structural stability of the interfaced domains, Tsu et al. [21] demonstrated experimentally the existence of chain-like objects on the surfaces of amorphous silicon viewed in high resolution microscopy. These chain-like objects could be the intersection with the surface of the domain interfaces. Tsu et al. have shown that the chain-like objects are 10-20 Å wide and hundreds of angströms long. It is interesting that the bond angle distortion is nearly zero in these objects, i.e. the configurations are in near crystalline state.

The atomic scale engineering of amorphous silicon will allow for getting amorphous domains doped by indium or arsenic, separated by crystalline angström-size interface. This feature suggests building a minimum size transistor p-i-n (see Fig. 6).

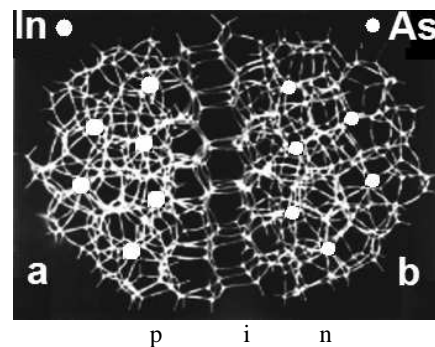


Fig. 6. The minimum size transistor made from two amorphous domains separated by a crystalline interface in silicon; a. the domain doped by indium (p-type); b. the domain doped by arsenic (n-type).

The aluminum electrodes and wires are important for the devices. Electron states formed from a combination of orbitals from the aluminum leads and silicon wire atoms penetrate all the way through nanowires of less than about one nanometer in length, giving such silicon bridges a finite conductance. But in longer structures, these electronic states penetrate only partially into the nanowire, with the silicon retaining its semiconducting properties. The transfer of electrons from the aluminum to the silicon at the junction between the two materials creates a localized dipole which forms a barrier to the flow

of electrons. The height of the barrier depends on the nature of bonding and atomic arrangement at the contact itself and varies for the various configurations of nano-wires.

The wave-like nature of the electrons could cause interference effects in the electrical conductance through the silicon nano-wires used as current channels. When voltage is applied to open the channel, electrons penetrating the silicon nano-wire from one of the aluminum leads may bounce off the contacts to the other lead and flow back toward the source contact. Upon reaching that contact, they may bounce off again, and the process may repeat itself. This behaviour results, at certain electron wavelengths and wire configurations, in interference resonances, leading to the occurrence of spikes in the current flowing through the nano-scale channel. These effects, as opposite to the macroscopic case, are in fact quantum effects interference resonances that appear during the movement of the electrons, and give rise to current spikes, that have impact on the functioning of the transistor.

2.5 Single molecule transistor

The last challenge in the miniaturization of the electron devices is the angstrom-size structure. The most interesting and flexible of these structures is basically a three-terminal transistor. There are source and drain contacts for sending current through the device, and the third terminal is a gate electrode. An applied voltage to the gate can alter the current from an "on-state" to an "off-state".

The new transistor consists of only a single molecule, approaching the ultimate limit of miniaturization. The operation principle of a single molecule transistor is fundamentally different. The recent experiments [22] have shown that the device characteristics of a carbon-based single-molecule transistor are completely governed by the laws of quantum mechanics.

The development of electronics based on molecules has been for decades a challenging problem. Two difficulties had to be surpassed: 1) the long molecules are either semiconducting or insulating; this is because one-dimensional electron system undergoes a Peierls transition related to a tiny rearrangement of the atoms; this rearrangement is precisely such that, for electrons, an energy gap is opened at the Fermi energy; fortunately, in long carbon-based molecule the Peierls transition is absent; the carbon tubules are conducting! 2) the attachment of electrical wires to a single molecule is a big problem; in the last years the mesoscopic physics has not only studied the fundamental quantum mechanical properties but also has developed fabrication techniques for attaching wires to small pieces of material.

In practice the metallic wires are fabricated with electron beam lithography. Then carbon nano-tubes are randomly laid down. Thereafter, in an atomic force microscope there are picked out those devices where a single nano-tube connects two metal stripes.

In the angstrom-size molecular transistor electrons occupy quantized orbitals, which correspond to discrete levels in the energy spectrum. The current from source to drain contacts is carried exclusively by electrons that have exactly these particular energies. If one adds an electron to the molecule, one needs to pay more than just the finite energy to occupy the next available molecular state. One must also pay a so-called charging energy to compensate for the extra elementary charge that the molecule now contains. Therefore, both quantization of charge and quantized molecular states govern the electronic properties of the molecular transistor. The energy required to add an electron to the molecule can either be supplied by the voltage source between the two current contacts or by the voltage applied to the gate terminal. These voltages are the spectroscopic tools in the determination of the charging energies and the molecular states.

These quantum effects were found in ultra-small quantum dots transistors. The present transport experiments on carbon tubules are well explained by the theory developed for quantum dots. The small-size single molecule transistor can operate at room temperature. In this transistor, a single electron makes the difference between an on-state and an off-state. In order to create a little electronic circuit we must integrate or couple different nano-tubes. A technical advantage is given by the fact that a kink in a nano-tube can change it from metallic to semiconducting [23]. So, one can imagine building a specific electronic circuit by stretching and bending a couple of nano-tubes here and there.

2.6 Local photostructural transformations and sensors thereupon

The chalcogenides are materials that exhibit outstanding properties in the non-crystalline state [24 – 79]. Illumination produces, generally, a red-shift of the absorption edge which increases the absorption. The photo-darkening can be reversed by thermal annealing near the glass transition temperature. Annealing actually starts after turning off the light and progresses with a wide spectrum of anneal energies.

During illumination we have the dynamic state with all the recombination-induced local bonding changes and atom motions. The microscopic processes driving the reversible and irreversible photo-structural changes are the same. The difference arises from the initial states. For both transformations (photo-darkening and photo-bleaching) there exists the same elemental photo-structural step. Photo-darkening results from the cumulative effect of many photo-structural steps, which decreases the medium range order and increases the lone pair interactions and, thereby, the width of the valence band. During illumination, the material is in a dynamic state which leads at high intensities to fluidity, diffusion and phase changes. The elementary step is sketched in Fig. 7, after Fritzsche [80]. Fig. 7 depicts the local structure before photo-excitation (a), the transient exciton or transient intimate valence alternation pair (IVAP) state (b), and the structure after recombination (c). One notices that atoms can move

over atomic distances during such elementary step. We are dealing with angström-scale shifts. Therefore, the photo-structural effects in chalcogenides are governed by structural modifications at the angström scale.

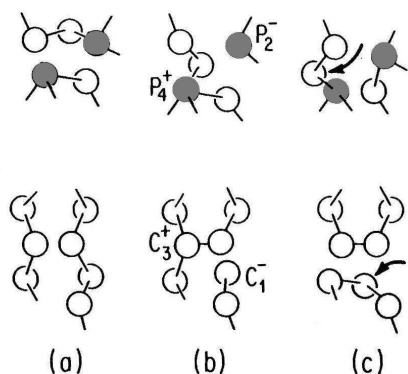


Fig. 7. The elementary step during photo-structural transformations. White balls are chalcogens and shaded balls are pnictide atoms. a. initial bonding configuration; b. transient self-trapped exciton after photon excitation; c. one of several new bonding configurations after recombination with motion of atoms indicated by arrow.

The light sensors can be developed on the base of the photodarkening/photobleaching effects in chalcogenide thin films [22a – 22d]. Because the elementary process is defined in a very narrow region of the chalcogenide glass (several angströms in diameter) then the device could work at the angström-scale.

2.7 Luminescence in fullerene-tubules configurations

The fullerene and tubule configurations of carbon can be combined in order to reach new complex configurations, where specific effects could be exploited.

Recently we have demonstrated that complex nano-tube + fullerene systems can be constructed without large distortions of the network of carbon atoms [4]. A combination fullerene C_{60} + low diameter angström-tubule was simulated.

Fig. 7 shows how a C_{60} fullerene cluster is linked to a nano-tubule of carbon. Thus the way is open for building entangled networks of tubes at the nano or angström level. In this way a complex circuit can be organized. Moreover, the fullerenes C_{60} contain a sufficient space to accommodate cluster of atoms (cluster of silicon of around 10-20 atoms, europium or erbium doped clusters). Thus the electro-luminescence of the clusters could be stimulated by controlling the current through the nano-tubes. A smart system can control the on- and off-state of the mini-lamps represented by clusters confined into the fullerene skeleton. The light emitted by the confined clusters could be sent to optoelectronic circuits.

The mechanism of structural connection between the two configurations fullerene and nano-tube has been

revealed [23a]. The connection is stable and deserves applications. Fig. 8a shows the intimate combinations of C_{60} fullerene and an angström-size nano-tubule after energy relaxation. The most interesting effect is the curving of the tube due to the intrinsic distortion forces acting longitudinally. The round conformation of the fullerene is modified around the connection region. Additionally, the circular section of the nano-tube is transformed into an ellipsoidal one (see Fig. 8b).

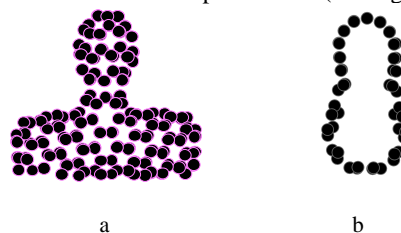


Fig. 8. Modeling of the connection between an angström-tubule and a C_{60} fullerene. a. interconnection; b. section in fullerene and in the tubule.

Now, by investigating the internal space occurring in fullerene and angström-tube (2.925 Å and 2.275 Å, respectively) it was shown that a small cluster or angström-dots can fill C_{60} (e.g. silicon, CdS or CdSe dots). In such a case the electroluminescent device is possible to be formed at the angström-scale. The tubes exhibit electrical conduction but the introduction of a row of metallic atoms can improve this property. The luminescent zones can be arranged in various positions, and, moreover, using the tubule-tubule connection in perpendicular directions, as already simulated by us (paper under preparation).

The small clusters or quantum dots are a sort of proto-solid. The proto-solids have both similitudes and differences with the macroscopic solids. Some clusters are “fluxional clusters” i.e. they can take various molecular configurations, as different isomers. Each isomer is locally stable because it economizes on energy but it may shift to a different isomeric form if enough energy is introduced through heating or light energy absorption.

Electronic configurations have a direct bearing on the frequency of various sizes because specific electronic bonding patterns make certain clusters particularly stable. These patterns depend on the orbitals from which the electrons originate and on the degree of freedom enjoyed by the electrons. When electrons are shared by the whole cluster in a delocalized cluster, so that negative charge is no greater at one point than another, the cluster may take on certain aspects of solid metal, such as conductivity. When the electrons are all tightly bound to atoms, the clusters resemble discrete molecules. Delocalized electrons are found in Na, K, and Cu, Ag clusters. These classes of metal atoms have a single electron in the “s” orbital that is then dispersed, or shared, among all the atoms in a given cluster. As the number of atoms in the cluster increases, the atomic orbitals combine to form molecular orbitals containing all the cluster’s electrons. The molecular orbitals then give way gradually to bands or energy states, akin to those of a solid. The information about the electronic configuration of clusters can be

gleaned from the amount of energy it takes to eject an electron from one of them. In the case of molecules, this energy requirement is called the ionization potential. For solids this energy is known as the work function. Lone atoms grip their electrons more tightly than clusters of atoms grip shared electrons, which is why most metals have ionization potentials about twice as high as their work functions. If clusters behave like bits of a solid, theory would predict a smooth, inverse relation between cluster size and electron-binding energy that would converge, at the limit, with the work function. It was found that the distance between two atoms of the smallest copper cluster is smaller than for larger clusters and for a big solid.

As a conclusion, when looking at the clusters it is important to have in mind: a. the electrons are in fact extended charge distributions, b. the bonds form when the overlap of different regions of electron charge surpasses a certain threshold, and c. the interaction between atoms is produced by charge redistributions and current flow.

Regarding the luminescence phenomenon in quantum dots, we must stress that this phenomenon occurs when an electron recombines with a hole to produce a photon. The probability that an electron-hole pair recombines by emitting a photon depends on the competition between radiative and non-radiative processes. Non-radiative recombinations include extrinsic processes such as recombination at bulk defects or surface dangling bonds and intrinsic phenomena such as Auger recombination. If fast, these processes can overwhelm radiative recombination. The only way to get good luminescence efficiencies in bulk silicon is to use very high purity material passivate the surface with great care, and electrically isolate it from the bulk, and keep the electron-hole density low enough to minimize Auger recombinations. In order to improve the light emission in silicon, there are two possibilities: i) to suppress the non-radiative recombination and ii) to enhance the radiative recombination. Using silicon quantum dots both conditions are fulfilled. The spatial localization of the electron and hole wave functions, in a dot of decreasing size, increases their spread in momentum space, hence increasing their overlap in the Brillouin zone. As a result the radiative recombination rate can increase by orders of magnitudes, bringing the radiative lifetime into the micro- or even nano-seconds time domain. For extremely small dots (<20 Å in diameter) direct recombination without phonon participation may even be favored over phonon-assisted recombination. On the other hand, quantum dots contain a small number of atoms (for 10 Å diameter, ~100 atoms and for 30 Å diameter, ~1000 atoms). The crystallographic imperfections, such as point defects or even dislocations that produce non-radiative recombinations, are unlikely to survive inside the quantum dot as they will move to the surface, where they are eliminated via surface reconstruction. Luminescence can originate from the silicon quantum dot itself, its surface or a luminescent center some distance away. In the first case, the exciton formed by the Coulombic attraction between an electron and a hole confined to the same dot disappears

by emitting a photon. The emitted photon energy is close to the band gap of the dot, which increases as the dot size decreases because of quantum confinement. The large surface to volume ratio of the dot (reaching up to 50 % atoms at the surface) requires that the surface be well passivated. One defect in quantum dots corresponds to an equivalent bulk concentration of $\sim 10^{20} \text{ cm}^{-3}$, which completely prevents the luminescence. In the second case a surface state captures the electron or the hole or both, where they recombine radiatively. In the third case, energy is transferred from the quantum dot to a luminescent center that can be located several angstroms or nanometers away. An important example is that of Erbium atoms in SiO_2 located in close proximity to a quantum dot. Energy transfer typically takes place on a microsecond time scale, leading to efficient luminescence near 1.54 μm wavelength.

The cathode-luminescence properties of the needle like structures (Ga_2O_3 , CdSe, SnO_2) have been recently investigated [81]. The luminescence is different from that in bulk material. In particular the internal faces of the nano-tube configurations of these compounds (obtained by heating the low particle size powders at temperatures higher as high as 900 °C in the case of CdSe; the needles form on the top of well-faceted rods and grow as hexagonal packing oriented along the c-axis, or develop dendrite growth) are highly luminescent. Nano-needles of Ga_2O_3 give rise to a new red luminescence band with some features which appear to be related to quantum effects. Needles of CdSe are associated with deep level cathode-luminescence emission in the range 1.65 – 1.75 eV, which is enhanced in specific parts of the structures as luminescent rings or on the internal surface of the tube.

2.8 Catalytical phenomena and application in fuel cells

The hydrogen energy conversion is efficiently performed in the fuel cells.

The classical fuel cells use aqueous (liquid) electrolytes and gas diffusion electrodes for the hydrogen oxidation and the oxygen reduction water producing process, in order to convert the chemical to electrical energy. Thus, the high amount of energy resulted from the combination of hydrogen and oxygen is converted, at least partially, in electricity. It is a three phase system, gas-liquid-gas, the phases being separated by the gas diffusion electrodes. Modern NAFION (perfluorosulphonic) membranes created by Dupont are widely used for proton exchange membranes in fuel cells. This is the most advanced and promising fuel cell version.

New proton conductive membranes could dramatically improve the performance of proton exchange membrane fuel cells [82].

Up to day catalyst carrier materials were the sub-micron carbon particles. Now fullerenes and carbon-tubes were suggested and applied. These materials could provide not only for a higher chemical and mechanical stability, higher electrical conductivity, but also, higher developed inter-phase boundary. A single angström-tube of carbon

will be loaded by catalyst clusters (Pt) (Fig. 9 a). A tube by itself would offer gas transport channels. The tube volume is almost inaccessible for other materials and cannot be filled except with gases. At the same time the walls apparently show a good permeability of atomic hydrogen. Long length tubes can be obtained (up to 10 micrometers). With such length, a tube can penetrate the entire reaction layer and will render good breathing conditions for the whole layer. If on the outer surface of the tubes, catalyst clusters are deposited (Fig. 9 b) and the fibers – catalyst loaded tube are embedded in a proton conductive polymer matrix forming a thin layer, then this layer can be easily sealed to a proton conductive membrane of the same material. Thus the proton exchange membrane can be double sided coated with a composite material of this kind to form the gas evolution and gas consuming reaction layers (Fig. 9 c). The integrated breathing reaction layer (Fig. 9 c) can effectively replace the gas diffusion – reaction layer double layer structure of catalyst coated membrane.

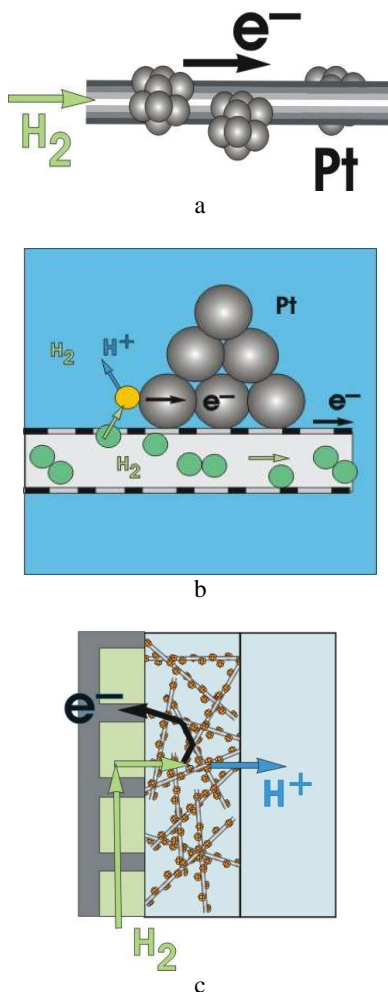


Fig. 9. The catalyst carried by an angström-size carbon-tube. a. carbon tubule loaded by platinum catalyst, with H_2 feeding; b. catalytic effect of platinum on single wall tubule; c. integrated breathing reaction layer in a electrode assembly.

The catalyst carrier being of the size of nanometers can bring additional nano-size effects. The distances between the catalyzed fibers are now so small that even if a catalyst particle has lost its direct contact with the carrier electron, tunneling can be expected making isolated catalyst particles effective. Hydrogen can be supplied in this case by the tubes and by short distance diffusion. Use of carbon nano-tubes such as nano-horns (Fig. 10) in fuel cell electrodes has been already reported [83].

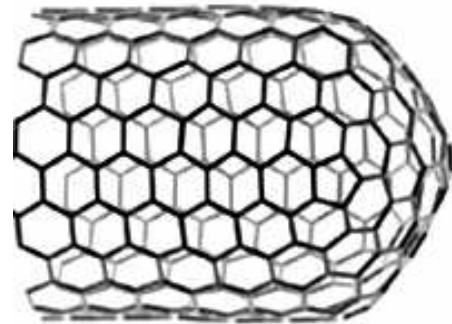


Fig. 10. The nanohorn structure.

2.9 Limit of lithography: Angström-lithography

Much of the tremendous progress in integrated circuits and technology and performance over the past 30 years has been fueled by the progress of lithography. The ability to print increasingly smaller features has enabled higher speed transistors, higher packing densities and lower power dissipation in CMOS circuits.

In the last decade excimer lasers have been introduced as light sources. KrF excimer lasers produce light in the deep ultraviolet (UV) at a wavelength of 248 nm. This source is used currently to produce the most advanced circuits with minimum design rules of 250 nm. Actually, the 248 nm deep UV is used to print the transistor gate features as small as 160 nm with Resolution Enhancement Technology (RET) which allows in some cases, printing of features somewhat below the conventional diffraction limit.

RET allow sub-diffraction printing by controlling the phase as well as amplitude of the light at the image plane in the printing system through the use of phase shifting masks. One other method uses pre-distorted amplitude patterns at the image plane to compensate for some diffraction effects (optical proximity effect correction (OPC)). Further, control of the distribution and angle of light (off-axis illumination, OAI) at the illumination aperture can accentuate higher diffraction orders leading to improved performance.

There are four leading candidates for next generation lithography technology: X-ray proximity, ultraviolet lithography, ion projection lithography and SCALPEL projection electron beam lithography.

A new lithography process was used in order to reach the limit of ~ 1 nm resolution. Using the porous alumina

templates, Qin et al. [84] deposited electrochemically a nano-wire comprising alternately, segments of Au then short segments of Ag or Ni (with length tailored by the deposition charge). The template is then dissolved, and an aqueous suspension of nano-wires cast onto a slide. The silicon dots act as a gutter-shaped support. Ni segments are then etched using nitric acid, leaving gaps. Au-Ag nano-wires are coated with Au/Ti bi-layer, and Ag etched away with a solution of CH_3OH , NH_4OH and H_2O_2 . The latest work has achieved 1 nm gaps [85].

Of high importance is the photo-resist used in lithography. The chalcogenide photo-resist (as e.g. glassy As_2S_3) is largely investigated and used. The photo-structural changes are induced at a larger scale and depend on the width of the used light beam. If the beam is correctly tuned, then, at its center of maximum intensity, a special phenomenon could be exploited: the formation of thin strips of chiral atomic configurations in the chalcogenide glass. The chiral configurations create anisotropy in the crystal and determine a very finely defined resistance to etching (positive photo-resist).

Recently, we approached the problem of the anisotropy in amorphous chalcogenides, with special emphasis on As_2S_3 glass, induced by light. We have demonstrated that the photon beam induces a chiral atomic configuration along the light propagation direction. The chiral chains into the non-crystalline network of e.g. As_2S_3 when nano-wires are considered, have been modeled in [86] (Fig. 11).

The chiral line can be tuned with high resolution. One chiral row of atoms comprises long chiral configurations of diameter extending down to minimum $2\div 3 \text{ \AA}$. The inscription resolution of the chiral lines into As_2S_3 glass depends on the laser beam concentration, but it is activated with more probability in the centre of the beam. Thus, a better resolution could be achieved at the angström-scale.

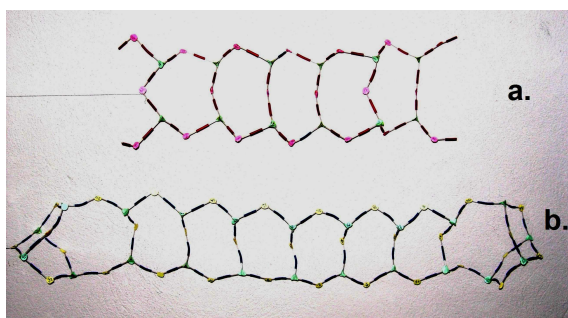


Fig. 11. Typical chiral, photoinduced configuration (a) and a non-chiral configuration (b) in As_2S_3 model.

2.10 Controlled drug release using a molecular valve

A reversible molecular valve that controls the release of molecules from angström-scale channels has been recently demonstrated [87]. One possible application of

the device is the controlled release of drugs from biochemical implants. The molecular valve is a rotaxane, which consists of a cyclic molecule or ring that is locked onto a dumbbell-shaped component. The ring has two separated recognition sites on the dumbbell and its position can be switched between the two sites by simple redox chemistry. In the ground state the ring is found at the tetrathiofulvalene (TTF) site. Oxidation of TTF destabilizes this configuration, and the ring moves to the dioxynaphthalene (DNP) site. Adding ascorbic acid returns the ring to the TTF site. The molecules were coupled to the surface of a silica support with $\sim 20 \text{ \AA}$ diameter tubular pores. When the rotaxane ring is near the pore opening, it blocks the pore, but when it moves away, the pore is unobstructed. In this way the rotaxane acts as a valve, controlling entry and exit from the silica pores. When the valve is open, the pores can be filled with guest molecules, in this case fluorescent dyes. Shutting the valve confines the dye in the pores.

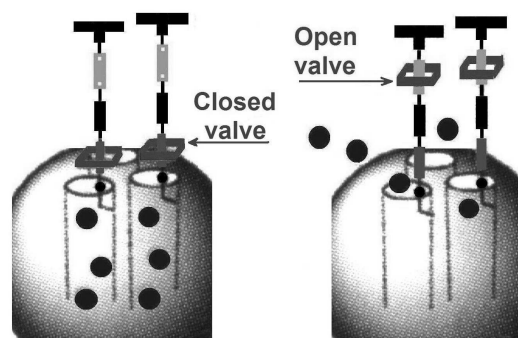


Fig. 12. Operation of the molecular valve [29].

The dye molecules can be released by simply adding ascorbic acid, and an immediate and fast increase in fluorescent intensity is observed. The process can be repeated, proving that this is a reversible machine controlled by simple redox chemistry (Fig. 12) [88]. The valve is truly reversible on the angström-scale. One of the most exciting application is the controlled release of insulin when the valve and the accompanying reservoir of drug are implanted directly in the body of a diabetic.

2.11 Molecular motors

The real-space realization of single-molecule rotors surrounded by like molecules that form a supramolecular bearing, have been already reported [89]. The single-molecule rotors are propeller-shaped units $\sim 1.5 \text{ nm}$ in diameter. In the molecular structure of hexa-tert-butyl decacyclene, the decacyclene core is equipped with six bulky t-butyl legs. Steric interactions between H atoms on the three outer naphthalene rings twist the molecule with respects to its central benzene ring, endowing it with a propeller form. These propeller molecules were deposited on atomically clean $\text{Cu}(100)$ surfaces. Given enough space the molecule rotates at high speed.

The molecular rotor works in a dry state and appears to be wearless. Its transition from the fixed to the rotating

states can be controlled locally by STM tip manipulation. The mass of the rotor is only 1.33×10^{-24} kg, leading to negligible inertia, and the rotor will stop instantaneously when the external drive is stopped.

Koumura et al. [90] reported a light-driven monodirectional molecular rotor. A repetitive, monodirectional rotation around a central carbon-carbon double bond in a chiral, helical alkene, with each 360° rotation involving four discrete isomerization steps activated by ultraviolet light or a change in the temperature of the system. First, the light induced trans to cis isomerization around a carbon-carbon double bond is an extremely fast and reversible process. In nature, it forms the basis for the information-retrieval step in the process of vision. Second, the concerted action of two chiral elements in a single chemical or physical event can lead to a unique handedness via the process of chiral discrimination, one of the essential features in living organisms. Steric interference in the molecule imposes a helical shape to the structure. Trans-1 and cis-2 are isomeric structures following a 180° rotation around the central bond, a process which is accomplished by irradiation with UV light at room temperature. The absorption of light energy and the unique combination of axial chirality and two chiral centres in this molecular rotor are essential for the observed monodirectional behaviour.

2.12 Molecular magnets and quantum computers

The future technology for designing computers is based on quantum mechanics. It uses the “qubit” or “quantumbit”, which can hold an impressive number of values. In 1996 such a computer was demonstrated by a joint group of scientists from the University of California and Stanford University.

The concept is that the atoms can be made to perform higher level gating functions rather than just to store “zero” and “1”. It is believed that such a device can handle multiple operations simultaneously in very large numbers, 10,000 times faster than today’s computers.

A quantum computer is any device for computation that makes direct use of distinctively quantum mechanical phenomena, such as superposition and entanglement to perform operations on data. Qubits for a quantum computer can be implemented using particles with two spin states “up” and “down”. There is a number of quantum computing candidates: i) superconduction based, ii) trapped in quantum computers, iii) electrons on helium q.c., iv) NMR – on molecules in solution, v) quantum dots on surface, vi) fullerene based ESR q.c., vii) quantum optics computer and, last but not least, molecular magnet – based q.c.

The molecular magnets are angström-size systems where a permanent magnetization and magnetic hysteresis can be achieved (although usually at extremely low temperatures) not through a three-dimensional magnetic ordering but as a purely one- molecule phenomenon.

The requisites for such a system are: a) a high spin ground state and b) a high zero-field-splitting (due to high magnetic anisotropy). The combination of these properties

can lead to an energy barrier, so that, at low temperatures, the system can be trapped in one of the high-spin energy wells. Molecular magnets exhibit an increasing product (magnetic susceptibility times temperature) with decreasing temperature, and can be characterized by a shift both in position and intensity of the a.c. magnetic susceptibility. The first molecular magnet was a dodecanuclear manganese complex, which is held together by oxo-bridges and acetate anions.

2.13 Self-organization as technological manipulation at the angström scale

Of course we need now the tools to be used for angstrom-technology. One key issue is forming discrete organized particles, as opposed to extended homogeneous arrays [91,92]. These discrete particles allow getting three-dimensional structures with various magnetic, electronic, and optical properties. These assemblies could be placed on the surfaces to create devices and sensors of several angstroms or ten of angstroms in diameters. A “mortar” with recognition element-functionalized polymers is used to assemble complementary particle “bricks” [93]. Other alternative is to trigger the formation of specific aggregates or atomic configurations in rather homogeneous matrices using the energy controlled self-assembling processes. The formation of discrete, regular atomic scale particles of controlled size and shape and spatial arrangement is an important step on the way to controlled particle assembly.

Self-assembly can be defined as “the process of self-organization of one or more entities as the total energy of the system is minimized to result in a more stable state”. The process of self-assembly inherently implies: a. some mechanism where movement of entities takes place using diffusion, electrical fields, etc... b. the concept of “recognition” between different elements that results in self-assembly, c. where the recognition leads to the binding of the elements dictated by forces (electrical, covalent, ionic, hydrogen bonding, van der Waals, etc...) such that the resulting physical placement of the entities pushes the system in the state of lowest energy.

Two key elements in molecular self-assembly are chemical complementarity and structural compatibility through weak and non-covalent interactions.

There is a continuous interest to develop concepts and approaches for self-assembled systems for electronic and optoelectronic applications. Material self assembly has been demonstrated in a variety of semiconductors (GaAs, InSb, SiGe...) using Stranski-Krastanov strain-dependent growth of lattice mismatch epitaxial films [94-97]. There is a high interest in assembling semiconductor transistors [98], carbon nanotubes [99,100] and quantum wires [101,13], which can be used as active devices for memory and logic applications, as already shown in this paper.

One approach is to design new materials through molecular self-assembly, which is ubiquitous in nature. Molecular self-assembly involves mostly weak and non-covalent bonds, which are individually quite insignificant. Collectively, however, these weak interactions, notably a)

hydrogen bonds, b) ionic bonds (electrostatic interactions, c) van der Waals interactions, d) hydrophobic interactions, e) water-mediated hydrogen bonds, play an indispensable role in all biological structures and their interactions. The water-mediated hydrogen bond is especially important for biological systems, because all such materials interact with water. For example in the structure of collagen these bonds are essentials for holding the three-stranded collagen helix together, both intra- and inter-molecularly.

It is possible to build nano- and angström- size structures and devices through molecular self-assembly and programmed molecular assembly.

The self-organization in silicon particles has been, recently, experimentally demonstrated. By heating the silicon to more than 1,100 degrees Celsius and cooling it repeatedly inside a nitrogen atmosphere, silicon begins to organize itself into ordered rows of crystallites, like bricks just a few atoms wide.

Terfort, Bowden and Whitesides [102] have shown that shape-selective recognition of surfaces and minimization of interfacial free energies can be combined to provide a strategy for assembling small components into three-dimensional assemblies. Because association is reversible, the system is self-repairing: formation of ever correctly assembled objects is possible. In such a case we will be able to build functional devices.

We must remark that at the nano or angström level all fields of science and engineering meet. Only the contribution of various achievements in low dimensional science, in quantum feature of the angström-phenomena, in atomic-scale manipulation, in molecular-scale self-organization, and in sub-nano-scale circuits will allow to the angström-technology to flourish in the not too far future.

3. Conclusions

The angström-scale behaviour is the "missing link" between atomic behaviour and nano-particle behaviour in solid matter. Angström-science is still in his infancy. Angström technology needs specific tools. Angström devices are not yet developed but a bright future is guessed beyond the horizon line of the modern technology. Rational manipulation techniques have to be further developed to enable integration of the prepared angström-objects into actual devices. From a more applied standpoint, the contact problem, i.e. the connection of the macroscopic and the molecular (atomic) worlds, and the design of highly parallel angström-fabrication processes constitute two important challenges in moving from angström-science to angström-technology. The self-organization that mimics the biomolecular organization seems to be the best approach to the formation of controlled angström-structures.

The angström devices need a protecting environment and this could be nothing else than big round carbon fullerenes or similar cage-like configurations. The carbon tubules will be used to control the connections between

devices and the general functionality of the angström-size optoelectronic integrated circuits.

Acknowledgement

The author kindly acknowledge the financial support in the frame of MATNANTECH CEEX project 4(501) 2005 and partially by CERES 4-118 2004 project.

References

- [1] H. W. Kroto, J. R. Heath, S. C. O'Brien, R. F. Curl, R. E. Smalley, *Nature* **318**, 162 (1985).
- [2] K. S. Novoselov, D. Jiang, F. Schedin, T. J. Booth, V. V. Khotkevich, S. V. Morozov, A. K. Geim, *Science* **306**, 666 (2004).
- [3] Andre K. Geim, *Materials Today*, December 2004, p. 7.
- [4] S. Iijima, *Nature* **354**, 56 (1991).
- [5] A. Lőrinczi, F. Sava, A. Anghel, *J. Optoelectron. Adv. Mater.* **6**(1), 349 (2004).
- [6] M. Popescu, F. Sava, A. Lőrinczi, Comm. to ECD Inc, Rochester Hills, Detroit, November 2004.
- [7] H. N. Postma, T. Tijs, Z. Yao, M. Grifoni, C. Decker, *Science* **293**, 76 (2001).
- [8] S. R. Ovshinsky, *Phys. Rev. Lett.* **21**, 1450 (1968).
- [9] D. Strand, J. Gonzalez-Hernandez, B. S. Chao, S. R. Ovshinsky, F. Gasiorowski, D. A. Pawlik, *Mat. Res. Soc. Symp. Proc.*, Vol. 230, 251 (1992).
- [10] A. Kolobov, P. Fons, A. I. Frenkel, A. L. Ankudinov, J. Tominaga, T. Uruga, *Nature Materials* **3**, 703 (2004).
- [11] W. Welnic, A. Pamunkgas, R. Detemple, C. Steimer, S. Bluegel, M. Wuttig, *Nature Materials*, 2005, p. 1
- [12] M. Popescu, F. Sava, A. Anghel, A. Lőrinczi, I. Kaban, W. Hoyer, *J. Optoelectron. Adv. Mater.* **7**(4), 1743 (2005).
- [13] C. M. Lieber, Y. Cui, *Science* **291**, 851 (2001).
- [14] G. Zheng et al. *Adv. Mater.* **16**(21), 1890 (2004).
- [15] Y. Wu et al., *Nano Letter.* **4**(3), 433 (2004).
- [16] A. B. Greytak, L. I. Lauhon, M. S. Gudiksen, C. M. Lieber, *Appl. Phys. Lett.* **84**(21), 4176 (2004).
- [17] R. M. Atlas, *Nat. Rev. Microbiol.* **1**, 70 (2003).
- [18] Y. Huang, Yu Huang, X. Duan, Y. Cui, L. J. Lauhon, Kyung-ha Kim, C. M. Lieber, "Logic Gates and Computation from Assembled Nanowire Building Blocks", *Science* **294**, 1313 (2001).
- [19] D. A. Muller, T. Sorsch, S. Moccio, F. H. Baumann, K. Evans-Lutterodt, G. Timp, *Nature* **399**, 758 (1999).
- [20] M. Popescu, *J. Non-Crystalline Solids* **192&193**, 140-144 (1991).
- [21] D. Tsu, B. S. Chao, S. J. Jones, *Solar Energy Materials & Solar Cells* **78**, 115 (2003).
- [22] R. C. Ashoori, *Nature* **380**, 559 (1996).
- [23] L. Kounwenhoven, *Science*, **268**, 1440 (1995).
- [24] D. Lezal, J. Pedlikova, J. Zavadil, *J. Optoelectron. Adv. Mater.* **6**(1), 133 (2004).

- [25] M. L. Trunov, V. S. Bilanich, *J. Optoelectron. Adv. Mater.* **6**(1), 157 (2004).
- [26] J. Kaluzny, D. Lezal, E. Mariani, J. Zavadil, *J. Optoelectron. Adv. Mater.* **6**(2), 421 (2004).
- [27] N. Mehta, M. Zulfequar, A. Kumar, *J. Optoelectron. Adv. Mater.* **6**(2), 441 (2004).
- [28] M. Stabl, L. Tichy, *J. Optoelectron. Adv. Mater.* **6**(3), 781 (2004).
- [29] J. Navratil, T. Plechacek, L. Benes, M. Vlcek, *J. Optoelectron. Adv. Mater.* **6**(3), 787 (2004).
- [30] K. Tanaka, T. Gotoh, K. Sugawara, *J. Optoelectron. Adv. Mater.* **6**(4), 1133 (2004).
- [31] T. Kavetskiy, R. Golovchak, O. Shpotyuk, J. Filipeki, J. Swiatek, *J. Optoelectron. Adv. Mater.* **6**(4), 1141 (2004).
- [32] M. Popescu, *J. Optoelectron. Adv. Mater.* **6**(4), 1147 (2004).
- [33] V. S. Kushwaha, A. Kumar, *J. Optoelectron. Adv. Mater.* **6**(4), 1159 (2004).
- [34] A. F. Petrović, S. R. Likić, D. D. Strbać, *J. Optoelectron. Adv. Mater.* **6**(4), 1167 (2004).
- [35] R. M. Holomb, V. M. Mitsa, *J. Optoelectron. Adv. Mater.* **6**(4), 1177 (2004).
- [36] N. Mehta, R. K. Shkula, A. Kumar, *J. Optoelectron. Adv. Mater.* **6**(4), 1185 (2004).
- [37] D. Platikanov, D. Arsova, E. Skordeva, *J. Optoelectron. Adv. Mater.* **7**(1), 337 (2005).
- [38] J. Dikova, Tz. Babeva, P. Sharlandjev, *J. Optoelectron. Adv. Mater.* **7**(1), 361 (2005).
- [39] M. Popescu, F. Sava, A. Lörinczi, D. Savastru, S. Mioclos, R. Savastru, *J. Optoelectron. Adv. Mater.* **7**(2), 1103 (2005).
- [40] A. Zakery, *J. Optoelectron. Adv. Mater.* **7**(3), 1143 (2005).
- [41] Y. C. Boulmetis, C. Raptis, D. Arsova, *J. Optoelectron. Adv. Mater.* **7**(3), 1209 (2005).
- [42] M. L. Trunov, *J. Optoelectron. Adv. Mater.* **7**(3), 1223 (2005).
- [43] V. Pamukchieva, A. Szekers, *J. Optoelectron. Adv. Mater.* **7**(3), 1277 (2005).
- [44] J. Dikova, Tz. Babeva, Tz. Iliev, *J. Optoelectron. Adv. Mater.* **7**(3), 1287 (2005).
- [45] J. Taseeva, K. Petkov, D. Kozhuharova, Tz. Iliev, *J. Optoelectron. Adv. Mater.* **7**(3), 1287 (2005).
- [46] P. Gushterova, P. Sharlandjev, *J. Optoelectron. Adv. Mater.* **7**(3), 1306 (2005).
- [47] V. I. Min'ko, I. Z. Indutnyy, *J. Optoelectron. Adv. Mater.* **7**(3), 1429 (2005).
- [48] D. Kumar, A. Kumar, *J. Optoelectron. Adv. Mater.* **7**(3), 1463 (2005).
- [49] G. Lukosky, *J. Optoelectron. Adv. Mater.* **7**(4), 1676 (2005).
- [50] G. Lucovsky, *J. Optoelectron. Adv. Mater.* **7**(4), 1277 (2005).
- [51] V. S. Minaev, S. P. Timoshenkov, V. V. Kalugin, *J. Optoelectron. Adv. Mater.* **7**(4), 1691 (2005).
- [52] P. J. Allen, B. R. Johnson, B. J. Riley, *J. Optoelectron. Adv. Mater.* **7**(4), 1759 (2005).
- [53] N. Qamhieh, G. J. Adriaenssens, *J. Optoelectron. Adv. Mater.* **7**(4), 1785 (2005).
- [54] R. Holomb, V. Mitsa, P. Johansson, *J. Optoelectron. Adv. Mater.* **7**(4), 1881 (2005).
- [55] I. I. Shpak, M. Kranjčec, I. P. Studenyak, *J. Optoelectron. Adv. Mater.* **7**(4), 2017(2005).
- [56] S. K. Tripathi, A. Thakur, G. Singh, *J. Optoelectron. Adv. Mater.* **7**(4), 2095 (2005).
- [57] M. Popescu, *J. Optoelectron. Adv. Mater.* **7**(4), 2189 (2005).
- [58] J. Hegedus, K. Kohary, S. Kugler, *J. Optoelectron. Adv. Mater.* **7**(5), 2231 (2005).
- [59] M. L. Trunov, *J. Optoelectron. Adv. Mater.* **7**(5), 2235 (2005).
- [60] N. P. Eisenberg, M. Manevich, A. Arsh, M. Klebanov, V. Lyubin, *J. Optoelectron. Adv. Mater.* **7**(5), 2275 (2005).
- [61] D. Lezal, J. Zavadil, M. Prochazka, *J. Optoelectron. Adv. Mater.* **7**(5), 2281 (2005).
- [62] M. Iovu, A. Andriesh, I. Culeac, *J. Optoelectron. Adv. Mater.* **7**(5), 2323(2005).
- [63] K. Tanaka, *J. Optoelectron. Adv. Mater.* **7**(5), 2571 (2005).
- [64] J. Teteris, M. Reinjelde, *J. Optoelectron. Adv. Mater.* **7**(5), 2581 (2005).
- [65] B. Georgieva, I. Podolesheva, J. Pirov, V. Platikanova, *J. Optoelectron. Adv. Mater.* **7**(5), 2595 (2005).
- [66] C. Vigreux – Bercovici, L. Lobadie, J. E. Broquin, P. Kern, A. Pradel, *J. Optoelectron. Adv. Mater.* **7**(5), 2625 (2005).
- [67] P. Němec, J. Jedelský, M. Fruma. M. Vlek, *J. Optoelectron. Adv. Mater.* **7**(5), 2635 (2005).
- [68] V. Pandey, N. Mehta, S. K. Tripathi, A. Kumar, *J. Optoelectron. Adv. Mater.* **7**(5), 2641 (2005).
- [69] P. sharma, M. Vashishta, I. P. Jain, *J. Optoelectron. Adv. Mater.* **7**(5), 2647 (2005).
- [70] A. Andriesh, *J. Optoelectron. Adv. Mater.* **7**(6), 2931 (2005).
- [71] J. Dikova, *J. Optoelectron. Adv. Mater.* **7**(6), 2945 (2005).
- [72] V. M. Kryshenik, V. P. Ivanitsky, V. S. Kavtuninko, *J. Optoelectron. Adv. Mater.* **7**(6), 2953 (2005).
- [73] P. Sharma, M. Vashishta, J. P. Jain, *J. Optoelectron. Adv. Mater.* **7**(6), 2963 (2005).
- [74] N. Mehta, D. Kumar, S. Kumar, A. Kumar, *J. Optoelectron. Adv. Mater.* **7**(6), 2971 (2005).
- [75] I. Ohlidal, D. Franta, M. Frumar, J. Jedelský, J. Omasta, *Chalc. Lett.* **1**(1), 1 (2004).
- [76] D. Lezal, J. Pedlikova, J. Zavadil, *Chalc. Lett.* **1**(1), 11 (2004).
- [77] M. L. Trunov, V. S. Bilanich, *Chalc. Lett.* **1**(2), 23 (2004).
- [78] M. A. Popescu, *Chalc. Lett.* **1**(12), 145 (2004).
- [79] A. Lörinczi, M. Popescu, F. Sava, A. Anghel, *J. Optoelectron. Adv. Mater.* **6**(1), 349 (2004).
- [80] H. Fritzsche, *Fiz. i Tehn. Poluprovod. (russ.) Tom* **32**(8), 452 (1998).
- [81] J. Piqueras, A. Cremades, P. Fernandez, D. Maestre, B. Mendez, E. Nogales, A. Urbietta, *Microscopy and Analysis*, **20**(1), 23 (2006).

- [82] E. Budevski, J. Optoelectron. Adv. Mater. **5**(5), 1319 (2003).
- [83] NEC Corporation, "NEC uses carbon nanotubes to develop a tiny fuel cell for mobile applications – A big step for next generation energy with nanotechnology", NEC, Tokyo, August 30, 2001.
- [84] L. Qin, S. Park, L. Huang, C. A. Mirkin, Science **309**, 113 (2005).
- [85] Materials Today, September 2005, p. 10.
- [86] M. Popescu, F. Sava, A. Lőrinczi, J. Non-Crystalline Solids, 2005, under print.
- [87] H. Nguyen et al., Proc. Natl. Acad. Sci. USA **102**, 10029 (2005).
- [88] J. Wood, Materials Today **8**(9), 13 (2005).
- [89] J. K. Gimzewski, C. Joachim, R. R. Schlittler, V. Langlais, H. Tang, I. Johanssen, Science **281**, 531 (1998).
- [90] N. Koumura, R. W. J. Zijlstra, R. A. van Delden, N. Harada, B. L. Feringa, Nature **401**, 152 (1999).
- [91] A. N. Shipway, E. Katz, I. Willner, Chem. Phys. Chem. **1**, 18 (2000).
- [92] C. B. Murray, C. R. Kagan, m. G. Bawendi, Annual. Rev. Mater. Sci. **30**, 545 (2000).
- [93] A. K. Boal, F. Ilhan, J. E. Derouchey, T. Thurn-Albrecht, T. P. Russell, V. M. Rotello, Nature **404**, 746 (2000).
- [94] A. Madhukar, Q. Xie, P. Chen, A. Konkar, Appl. Phys. Lett. **64**(20), 2727 (1994).
- [95] J. M. Moison, F. Houzan, F. Barthe, L. Leprince, E. André, O. Vatel, Appl. Phys. Lett. **64**(2), 196 (1994).
- [96] T. I. Kamins, E. C. Carr, R. S. Williams, S. J. Rosmet, J. Appl. Phys. **81**(1), 211 (1997).
- [97] R. Bashir, A. E. Kabir, K. Chao, Applied Surf. Sci., **152**, 99 (1999).
- [98] The International Technology Roadmap for Semiconductors (NTRS), SIA 1997 and 1999.
- [99] V. Derycke, R. Martell, J. Appenzeller, Ph. Avouris, Nanoletters **1**(9), 453 (2001).
- [100] J. Liu, M. J. Casavant, M. Cox, D. A. Walters, P. Boul, Wei Lu, A. J. Rumberg, K. A. Smith, Daniel T. Colbert, Richard E. Smalley, Chemical Physics Letters **303**, 125 (1999).
- [101] Y. Huang, X. Duan, Q. Wei, C. M. Lieber, Science **291**, 630 (2001).
- [102] A. Terfort, N. Bowden, G. M. Whitesides, Nature, **386**, 162 (1997).

Corresponding author: mpopescu@infim.ro